semiconductor heterojunctions is important in order to describe their electric properties as well as to design a heterojunction-bipolar transistor (HBT) with a wide-bandgap emitter.[1] As is clear from the energy-band diagram shown in Fig. 3.6, the energy difference between the conduction band in a-Si:H and the Fermi level at the interface is expressed as $qV_{B2}+\delta_2$ in the a-Si:H side and $\Delta E_C-qV_{B1}+E_{g1}-\delta_1$ in the c-Si side. Therefore, ΔE_C is expressed by

$$\Delta E_C = \delta_1 + \delta_2 - E_{g1} + qV_B \quad . \tag{3-12}$$

On the other hand, ΔE_C is defined as

$$\Delta E_C \equiv \chi_1 - \chi_2 \quad . \tag{3-13}$$

Experimentally, the value of δ_1 is estimated from N_A as shown in Table 3-1 and the value of δ_2 is the same as the activation energy of dark conductivity of a-Si:H. By substituting quantitative data on δ_1, δ_2, χ_1, E_{g1}, and V_B to Eqs. (3-12) and (3-13), the values of ΔE_C and χ_2 are determined as

$$\Delta E_C = 0.20 \pm 0.07 \text{ eV}$$

and

$$\chi_2 = 3.85 \pm 0.07 \text{ eV} \quad ,$$

using E_{g1}=1.12 eV and χ_1=4.05 eV.[9] Figure 3.10 shows the energy-band diagrams for the diodes (samples 5-8) with four different p c-Si resistivities, sketched on the basis of the above results.

3-3. Simulation of High-frequency C-V Characteristics

3-3-1. Modeling

Though only the undoped (i.e., slightly n-type) a-Si:H/p c-

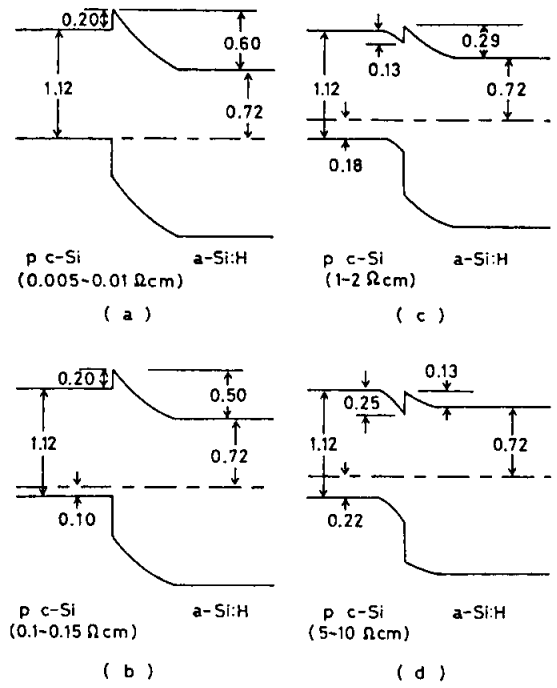

Fig.3.10. Energy-band diagrams in interface regions for heterojunctions using p c-Si with different resistivities. Resistivities of p c-Si are (a) 0.005-0.01 Ω cm, (b) 0.1-0.15 Ω cm, (c) 1-2 Ω cm, and (d) 5-10 Ω cm.

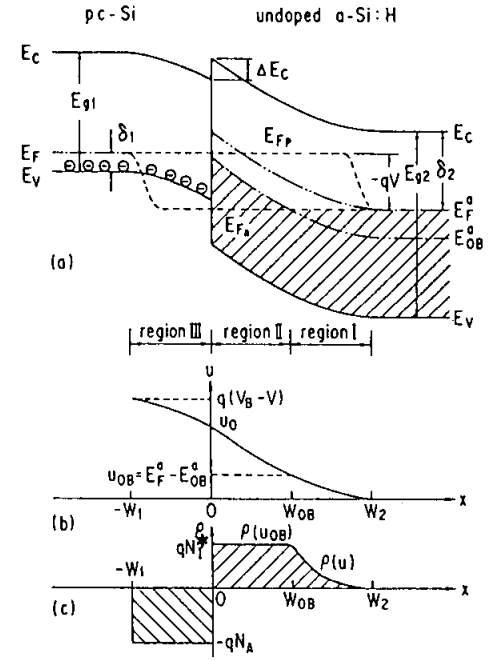

Fig.3.11. Schematic sketches of p c-Si/undoped a-Si heterojunction: (a) energy-band diagram, (b) energy variation for electron, and (c) space-charge density variation for dc reverse-bias voltage condition. Gap states indicated by hatched area of (a) are occupied by electrons.

Si heterojunction is considered in this section, it is easily able to expand this discussion into a general discussion about highly resistive amorphous/lowly resistive crystalline semiconductor heterojunctions. Although there are reports on the simulation of the zero-frequency C-V characteristics of those heterojunctions,[10-13] there is no report on that of the high-frequency C-V characteristics. Here, the following models for simulating the C-V characteristics of the heterojunction are adopted;

(1) one kind of g(E) in undoped a-Si:H, instead of two kinds of g(E) [i.e., donorlike g(E) and acceptorlike g(E)], because it is unnecessary to classify g(E) into two kinds of g(E) as is getting clear from the following discussion;

(2) a carrier occupation function for gap states in the depletion region, which is derived from emission rates for electrons and holes, instead of the Fermi-Dirac distribution function, because the heterojunctions exhibit good rectifying properties in current-voltage (I-V) characteristics, which is quite different from the MOS diodes.

Figure 3.11 shows an energy-band diagram, an energy variation [u(x)] for electrons, and space charges produced by the dc reverse bias (V) for such a heterojunction. When V is applied across the heterojunction, the depletion regions in both a-Si:H and c-Si are formed as shown in Fig. 3.11(a). Because a-Si:H has continuous distribution of the gap states, the spatial distribution of the space charge in the a-Si:H depletion region is not simple. The difference between the a-Si:H depletion region ($0 \leqq x \leqq W_2$) and the neutral region ($x \geqq W_2$) is based on:

1. Whether electrons exist at gap states between E_F and E_{OB};
2. Whether electrons exist in the conduction band as well as in the conduction-band tail.

These changes will result in the formation of the positive space charge in the depletion region of a-Si:H. In this analysis, therefore, charged states (e.g., shallow donors) in both neutral and depletion regions need not be explicitly considered.

In the neutral region, for instance, the electron concentration (n) in the conduction band of undoped a-Si:H is about 6×10^{9} cm^{-3}, which is calculated using the relation $\sigma_2=q\mu_2 n$, where the dark conductivity (σ_2) is 10^{-9} S/cm, the electron charge (q) is 1.6×10^{-19} C, and the drift mobility (μ_2) is 1 $cm^2V^{-1}s^{-1}$. Since this value is much smaller than the expected space-charge density ($\geq 10^{15}$ cm^{-3}, which is the experimentally obtained value of N_I) in the depletion region of undoped a-Si:H, the contribution of the electrons in the conduction band to the production of the space charge can be neglected.

The electron density (n_{BT}) in the conduction-band tail can be estimated as

$$n_{BT} = \int_{E_F^a}^{E_C} f(E)N(E_C)\exp[-(E_C - E)/E_{BT}]dE \quad , \qquad (3\text{-}14)$$

where f(E) is the Fermi-Dirac distribution function, $N(E_C)$ is the density at the bottom of the conduction band, E_F^a is the Fermi level in the neutral region of a-Si:H, and E_{BT} is the characteristic energy for the conduction-band tail of a-Si:H. The value of n_{BT} is 2×10^{13} cm^{-3} using $N(E_C)=10^{21}$ $cm^{-3}eV^{-1}$, $(E_C-E_F^a)=0.73$ eV, and $E_{BT}=50$ meV, suggesting that the contribution of the electrons in the conduction-band tail to the production of the space charge can be also neglected. Since E_{BT} of 50 meV is overestimated (i.e., E_{BT} is usually considered to be smaller than 40 meV),[14] other gap states above E_F must be hidden by the assumed conduction-band tail states. Therefore, the change of occupation at the gap states below the Fermi level mainly produces the positive space charge in the depletion region.

The electron occupation at gap states in the depletion region is governed by a balance between the thermal emission process and the capture process of electrons and holes between gap states and the extended states.[15,16] It is useful to consider one particular energy level (E_{OB}) at which the thermal-emission rate for electrons equals that for holes in the following discussion.

The quasi-Fermi level of electrons (E_{Fn}) is almost constant in the whole depletion region and rises toward the Fermi level near the edge of the depletion region in p c-Si, while the quasi-Fermi level of holes (E_{Fp}) falls near the edge of the depletion region in a-Si:H, as shown in Fig. 3.11(a). The concepts of E_{Fn} and E_{Fp} are important to calculate the carrier densities in the extended states. On the other hand, the concept of the occupation function is important to estimate the trapped carrier density at gap states especially between E_{Fn} and E_{Fp}. The value of E_{OB} in a-Si:H is given by (See Appendix)

$$E_{OB} = E_V + E_{g2}/2 + (kT/2)\ln(\nu_p/\nu_n) \quad , \qquad (3\text{-}2)$$

and the states above E_{OB} are approximately considered to be empty of electrons while the states below E_{OB} are approximately considered to be full of electrons, as long as $E_{OB}>E_{Fn}$. Here, k is the Boltzmann's constant, T is the absolute temperature, E_V is the top of the valence band of a-Si:H, E_{g2} is the energy bandgap of a-Si:H, and ν_n and ν_p are the pre-exponential factors of thermal-emission rates (i.e., attempt-to-escape frequencies) for electrons and holes at the gap states, respectively.

Now considered is the space charge in the two depletion regions (region Ⅰ and region Ⅱ) of a-Si:H which are divided by the cross point (W_{OB}) at $E_{Fn}=E_{OB}$. In region Ⅰ ($W_{OB} \leqq x \leqq W_2$), where E_{Fn} is above E_{OB}, the space-charge density (ρ_I) at the spatial position (x) is expressed as

$$\rho_I[u(x)] = \int_{E_F^a - u(x)}^{E_F^a} g(E)dE \quad , \qquad (3\text{-}15)$$

where u(x) is the energy variation shown in Fig. 3.11(b), E_F^a is the Fermi level in the neutral region, and g(E) is the density-of-state distribution in a-Si:H. Here, for simplicity, the Fermi-Dirac distribution function and the electron occupation function for gap states are approximated by step functions.

In region Ⅱ ($0 \leqq x \leqq W_{OB}$), where E_{Fn} is below E_{OB}, the space-charge density is kept constant and is expressed as

$$\rho_I(u_{OB}) = \int_{E_F^a - u_{OB}}^{E_F^a} g(E)dE \qquad (3\text{-}16)$$

and

$$qN_I^* = \rho_I(u_{OB}) \qquad (3\text{-}17)$$

with

$$u_{OB} = E_F^a - E_{OB}^a \quad , \qquad (3\text{-}18)$$

where u_{OB} is the energy variation at $x=W_{OB}$, N_I^* is the density of midgap states between E_F^a and E_{OB}^a in a-Si:H, E_{OB}^a is E_{OB} in the neutral region of a-Si:H. At thermal equilibrium (i.e., V=0 V), when the built-in potential for a-Si:H is larger than the value of $(E_F^a - E_{OB}^a)/q$, $\rho_I(x)$ near the interface exceeds qN_I^* because the Fermi level is below E_{OB} near the interface. This situation near the interface remains the same even when the reverse bias is applied. However, as will be discussed later, the contribution of the excess charges near the interface can be included in the effect of charged states in the near-interface region.

In the depletion region in p c-Si, which is region Ⅲ ($-W_1 \leq x \leq 0$) in Fig. 3.11, the space-charge density is given by $-qN_A$ under the reasonable assumption that the p c-Si has only shallow acceptors whose density is N_A. As a consequence, the space-charge density can be schematically shown in Fig. 3.11(c).

3-3-2. Simulation

Based on the energy-band diagram mentioned above, the C-V characteristics of the amorphous/crystalline semiconductor heterojunction is theoretically considered. Simulations of the C-V characteristics of the amorphous/crystalline semiconductor heterojunctions at 0 Hz were reported,[10-13] but it is experimentally difficult to measure their very low frequency C-V characteristics that would correspond to the simulation data. Moreover, the experimental low frequency C-V characteristics vary with the measuring frequency due to the dielectric relaxation and